JOURNAL OF AGRICULTURAL AND FOOD CHEMISTRY

Article

Cite This: J. Agric. Food Chem. 2018, 66, 12206−12216

pubs.acs.org/JAFC

Nontargeted Metabolomic Study on Variation of Phenolics in Different Cranberry Cultivars Using UPLC-IM − HRMS

Yifei Wang,[†] Nicholi Vorsa,[‡] Peter de B. Harrington,[§] and Pei Chen*[,†]

[†]U.S. Department of Agriculture, Agricultural Research Service, Beltsville Human Nutrition Research Center, Food Composition and Methods Development Laboratory, Beltsville, Maryland 20705, United States

[‡]Philip E. Marucci Center for Blueberry and Cranberry Research and Extension, Rutgers University, Chatsworth, New Jersey 08019, United States

[§]Center for Intelligent Chemical Instrumentation, Department of Chemistry & Biochemistry, Ohio University, Athens, Ohio 45701, United States

Supporting Information

ABSTRACT: The metabolomic profiles of American cranberry (*Vaccinium macrocarpon*) fruits and their variation among 10 diverse cultivars were investigated by ultraperformance liquid chromatography ion-mobility high-resolution mass spectrometry (UPLC-IM − HRMS). Over 80 metabolites, belonging to various phenolic compound groups, were putatively characterized. An HRMS data matrix consisting of 4778 unique ions across the 10 cultivars was built and analyzed by orthogonal projections to latent structures discriminant analysis (OPLS-DA). The 10 cultivars segregated into 4 clusters on the basis of their metabolomic similarities, which largely reflected their genetic backgrounds. Anthocyanins exhibited the most extensive variations among all the cultivars, reflecting the effects of cranberry breeding selection on fruit color. Flavonols, phenolic acid derivatives, and proanthocyanidins also varied among the different cultivars. The nontargeted metabolomic comparison using multivariate analysis proved to be efficient and robust for determining specific metabolite differences among the cultivars.

KEYWORDS: *cranberry, UPLC, HRMS, phenolics, chemometrics, OPLS-DA*

INTRODUCTION

American cranberry (*Vaccinium macrocarpon* Ait.), together with blueberry (*Vaccinium* spp.) and native grape (*Vitis* spp.), are the three fruit crops native to North America. Cranberries are primarily produced in Wisconsin, Massachusetts, New Jersey, Oregon, and Washington of the US and several provinces of Canada.[1] In 2017, the US cranberry production was 837 million pounds with a total value of over $252 million (USDA-NASS, 2018). In recent years, cranberry has received growing research interest for its potential human health benefits. In particular, cranberry phenolic compounds, including flavonoids, phenolic acids, and other nonflavonoid polyphenols (e.g., resveratrol), have been reported to possess various health benefit effects such as antibacterial, anti-inflammatory, antioxidant, anticancer, and cardiovascular benefits and neural function protection.[2−5]

Cranberry has a relatively recent cultivation history in comparison to other crop species. It was first domesticated in the early 1800s in Massachusetts.[6] For 100 years or so, commercially grown cranberries were predominantly cultivars from wild selections, including "Early Black", "Howes", "McFarlin", and "Searles". The first cranberry breeding program was started by the USDA in 1929, with a major focus on developing varieties that are resistant to false-blossom disease, along with other favored traits such as good fruit color and high yield.[7] Six varieties were released from the program, including the most widely planted cultivar "Stevens".[8] Some cultivars were not officially named or released but have been commercially grown, such as '"No. 35". In 1985 and 1990, two cranberry breeding programs were established at Rutgers University (NJ) and the University of Wisconsin—Madison (WI). In 2003, the WI program released its second-generation hybrid cultivar "HyRed", marked with deep fruit color and early ripening.[9] Three cultivars were released by the Rutgers program in 2006, including "Crimson Queen", "Demoranville", and "Mullica Queen".[6] In comparison to first-generation hybrids, these cultivars had further improved fruit appearances and yields.

The effects of agricultural breeding on the secondary metabolites in crops have become a major research concern, due to the emerging evidence of their potential health benefits. Secondary metabolites carry critical functions for plants' survival and adaptation to different environmental conditions, and their production can be altered during the breeding process.[10] Several studies have reported variations of anthocyanin, flavonol, proanthocyanidin, or nonphenolic organic acid levels in different cranberry cultivars,[11−14] suggesting significant varietal effects on the accumulation of cranberry secondary metabolites. While these studies offer valuable information, the compounds in the reports were limited to preselected target metabolites and the diversity of cultivar selections was also limited for comprehensive evaluation. There is a lack of studies on full-scale profiling

Received: September 14, 2018
Revised: October 24, 2018
Accepted: October 29, 2018
Published: October 29, 2018

DOI: 10.1021/acs.jafc.8b05029
J. Agric. Food Chem. 2018, 66, 12206−12216

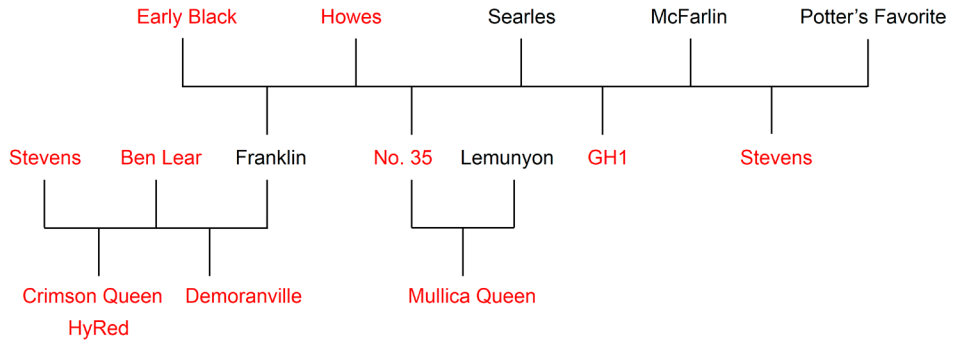

Figure 1. Pedigree tree of different cranberry cultivars. Cultivars analyzed in the study are marked in red.

and nontargeted metabolomics comparison of cranberry secondary metabolites in different cultivars.

Mass spectrometry has been the tool of choice for nontargeted metabolomics studies and generates informative but complex data sets. Chemometric tools such as principal component analysis (PCA), projection to latent structures (PLS), and orthogonal PLS (OPLS) offer efficient and robust interpretation and visualization of complex chemical data.[15] Using such approaches, Brown et al. evaluated the phytochemical diversity of five cranberry cultivars, without characterization of significant metabolites.[14] In the current study, 10 cranberry cultivars consisting of wild selections and first- and second-generation hybrids were analyzed by ultraperformance liquid chromatography coupled with ion-mobility and high-resolution mass spectrometry (UPLC-IM–HRMS). The aim of the study was to (1) comprehensively characterize cranberry secondary metabolites based on their LC and MS spectra and (2) systematically evaluate the metabolomic similarities and variations in diverse cranberry cultivars.

MATERIALS AND METHODS

Plant Materials. Fully ripe cranberry fruits were harvested from field plots at the P. E. Marucci Center for Blueberry and Cranberry Research and Extension at Chatsworth, NJ in September 2017. Ten cranberry cultivars were analyzed, including the three native selections "Howes" (HO), 'Early Black '(EB) and "Ben Lear" (BL), the two first-generation hybrids "Stevens" (ST) and "No. 35" (35), and the five second-generation hybrids "Crimson Queen" (CQ), "Demoranville" (DM), "Mullica Queen" (MQ), "HyRed" (HYR), and "GH1" (GH). Their genetic relationships are given in Figure 1. Cranberry plots were established in a randomized complete block design (RCBD) with four field replications. Fruits were kept at −20 °C until preparation.

Sample Preparation and Extraction. Frozen cranberry fruits were first lyophilized in a Labconco Bulk Tray Dryer (Kansas City, MO, USA) and then powdered. Cranberry powders (100 mg) were weighed to 0.1 mg, mixed with 5 mL of 70% methanol in 15 mL centrifuge tubes, sonicated for 45 min at room temperature, and centrifuged at 5000*g* for 10 min. Supernatants were collected and filtered through a 0.45 μm PVDF syringe filter (VWR Scientific, Seattle, WA, USA) prior to UPLC-HRMS analysis.

UPLC-HRMS Apparatus and Conditions. The UPLC-IM–HRMS analysis was carried out in a Waters ACQUITY UPLC I-Class system (binary solvent manager, sample manager, column heater and PDA eλ detector) coupled with a Waters Vion Ion Mobility Quadrupole Time of Flight (IMS QTof) mass spectrometer (Waters Corp., Milford, MA, USA). A Hypersil GOLD aQ column (200 × 2.1 mm, 1.9 μm particle size, ThermoFisher Scientific, Waltham, MA) was used for chromatographic separation. Mobile phase A was water with 0.1% formic acid, and mobile phase B was acetonitrile with 0.1% formic acid. The elution gradient was 4–18% B between 0 and 35 min, 18–35% B between 35 and 40 min, 35–95% B between 40 and 41 min, and 95% B between 41 and 52 min with a flow rate of 0.3 mL/min. The column was kept at 60 °C and equilibrated with 4% B for 6 min between injections. The injection volume was 1 μL.

IM HRMS data was acquired in high-definition MS^E mode, using the following parameters: ion source, ESI negative ion; analyzer type, sensitivity; source temperature, 100 °C; desolvation temperature, 400 °C; cone gas flow, 50 L/h; desolvation gas flow, 850 L/h; capillary voltage, 2.50 kV; low collision energy, 6.0 eV; high collision energy, 15.0–45.0 eV; mass range, 50–2000 m/z; scan rate, 0.25 s. Leucine encephalin (50 pg/mL, 10 μL/min) was used for lock mass correction at 0.25 min intervals. MS^E allows simultaneous acquisition of high-resolution mass data at both low and high collision energy and provides both precursor and fragment ion data in one analysis. MS and ion mobility data were acquired and processed in UNIFI (Waters Corp.). Two repeated analysis of 40 samples (10 cultivars × 4 biological replications) generated 80 acquisitions.

Data Processing for Chemometric Analysis. The raw data of the 80 acquisitions were exported into Progenesis QI software (Nonlinear Dynamics, Newcastle, U.K.) for advanced data processing. The step includes automatic peak alignment, peak peaking, and ion deconvolution. The retention time range was set between 3.5 and 42 min. A total of 4778 unique ions were detected across all samples and were exported into a two-dimensional 80 × 4778 (samples × mass peaks) matrix in Excel. Each mass peak in the matrix was associated with retention time, accurate mass, and ion mobility data.

Multivariate Analysis. The mass spectral data matrix was imported into SIMCA software (Version 14, Umetrics, Umeå, Sweden) for supervised orthogonal projections to latent structures discriminant analysis (OPLS-DA). Prior to analysis, variables were centered and scaled to pareto variance (i.e., mean-centering the variables followed by scaling by the square root of the standard deviation). A score plot of OPLS-DA was generated to visualize sample clustering. S-plots from OPLS-DA models were used for determining variable influence.

RESULTS AND DISCUSSION

Identification of Cranberry Secondary Metabolites. Typical UPLC chromatograms of cranberry samples at absorbances of 278 and 354 nm are presented in Figure S1 (Supporting Information). The 10 cultivars exhibited similar UPLC/PDA/MS chromatograms. Major compound peaks were putatively identified by their accurate masses (compound formula), MS fragmentation patterns, retention times, UV–vis absorbance, previous publications, and available reference standards. Most of the identified compounds were phenolic compounds, with the primary UV absorbance bands at 230–300 and/or 305–390 nm resulting from aromatic rings.[16] A total of 82 peaks were putatively identified (Table 1), mainly consisting of benzoic acid derivatives, hydroxybenzoic acid derivatives, hydroxycinnamic acid derivatives, flavonol glycosides, proanthocyanidins, and anthocyanins.

DOI: 10.1021/acs.jafc.8b05029
J. Agric. Food Chem. 2018, 66, 12206–12216

Table 1. UPLC-HRMS Data of Cranberry Compounds

peak	R_t (min)	$[M - H]^-$ or $[M - 2H]^{2-}$	formula	error (ppm)	major fragment ions[a]	tentative identification[b]
1	4.69	167.0346	$C_8H_8O_4$	−2.1	152(100), 108(75)	vanillic acid
2	4.81	299.0769	$C_{13}H_{16}O_8$	−1.1	179(100), 137(71), 93(65)	hydroxybenzoic acid glucoside
3	4.99	315.1081	$C_{14}H_{20}O_8$	−1.3	153(32), 123(100)	hydroxytyrosol glucoside
4	6.27	862.1738 (−2H)	$C_{90}H_{70}O_{36}$	−2.3	NA	A-Type PAC DP-6 (A = 2)
5	6.39	325.0926	$C_{15}H_{18}O_8$	−1	163(100), 119(90)	coumaric acid glucoside
6	6.66	503.141	$C_{21}H_{28}O_{14}$	0.6	341(100), 179(50), 161(48)	glucosyl-caffeoyl-glucose
7	6.93	341.0876	$C_{15}H_{18}O_9$	−0.5	179(8), 161(100), 133(31)	caffeoyl-glucose
8	7.23	163.0398	$C_9H_8O_3$	−1.8	119(100)	coumaric acid (a)
9	7.71	1151.2449	$C_{60}H_{48}O_{24}$	−1.2	863(100), 711(29)	A-Type PAC DP-4 (A = 1) (a)
10	8.02	577.135	$C_{30}H_{26}O_{12}$	−0.3	407(100), 289(45)	B-Type PAC DP-2 (a)
11	8.64	719.1501 (−2H)	$C_{75}H_{60}O_{30}$	−2.6	NA	A-Type PAC DP-5 (A = 1) (a)
12	8.85	289.0712	$C_{15}H_{14}O_6$	−2	245(100), 203(67)	catechin
13	9.05	445.1349	$C_{19}H_{26}O_{12}$	−0.5	323(84), 121(100)	benzoyl-hexosyl-hexoside (a)
14	9.33	341.0875	$C_{15}H_{18}O_9$	−0.8	179(33), 135(100)	caffeic acid glucoside
15	9.52	431.156	$C_{19}H_{28}O_{11}$	0.4	303(100), 269(70)	benzyl-hexosyl-hexoside
16	9.78	163.0397	$C_9H_8O_3$	−2.1	119(100)	coumaric acid (b)
17	10.15	325.0927	$C_{15}H_{18}O_8$	−0.5	145(100), 117(33)	coumaroyl-glucose (a)
18	10.35	353.0875	$C_{16}H_{18}O_9$	−0.7	191(100)	chlorogenic acid
19	10.68	719.1507 (−2H)	$C_{75}H_{60}O_{30}$	−1.8	573(80), 289(100)	A-Type PAC DP-5 (A = 1) (b)
20	10.89	121.0294	$C_7H_6O_2$	−0.9	77(100)	benzoic acid
21	11.1	325.0927	$C_{15}H_{18}O_8$	−0.4	145(100), 117(48)	coumaroyl-glucose (b)
22	11.66	461.1301	$C_{19}H_{26}O_{13}$	0.2	415(48), 121(100), 77(31)	hydroxybenzoyl-hexosyl-hexoside
23	11.99	445.1352	$C_{19}H_{26}O_{12}$	0	323(68), 121(100)	benzoyl-hexosyl-hexoside (b)
24	12.27	223.0609	$C_{11}H_{12}O_5$	−1.2	208(57), 164(60), 149(100)	sinapic acid
25	12.75	577.1346	$C_{30}H_{26}O_{12}$	−1	407(100), 289(31)	B-Type DP-2 (b)
26	12.9	355.1031	$C_{16}H_{20}O_9$	−1	175(45), 160(100), 132(42)	feruloyl-glucose
27	13.13	415.1244	$C_{18}H_{24}O_{11}$	−0.4	293(26), 121(100)	benzoyl-pentosyl-hexoside
28	13.32	719.1499 (−2H)	$C_{75}H_{60}O_{30}$	−2.9	289(100)	A-Type PAC DP-5 (A = 1) (c)
29	13.96	289.0714	$C_{15}H_{14}O_6$	−1.1	245(74), 203(100)	epicatechin
30 a	14.51	385.1139	$C_{17}H_{22}O_{10}$	−0.2	205(87), 190(100)	sinapoyl-glucose
30 b	14.51	719.1505 (−2H)	$C_{75}H_{60}O_{30}$	−2	863(25), 575(100)	A-Type PAC DP-5 (A = 1) (d)
31	15.05	385.1866	$C_{19}H_{30}O_8$	−0.4	205(65), 153(100)	unknown
32	15.28	1153.2602	$C_{60}H_{50}O_{24}$	−1.5	863(66), 577(81), 575(100)	B-type PAC DP-4
33	15.65	371.0985	$C_{16}H_{20}O_{10}$	0.2	249(100)	3-(benzoyloxy)-2-hydroxypropyl glucopyranosiduronic acid
34	15.9	1006.2042 (−2H)	$C_{105}H_{82}O_{42}$	−3.3	NA	A-Type PAC DP-7 (A = 2) (a)
35	17.31	461.1092 (−2H)	$C_{22}H_{23}O_{11}^+$	0.5	299(78), 298(100)	peonidin-3-galactoside
36a	18.06	863.1816	$C_{45}H_{36}O_{18}$	−1.4	711(49), 411(100), 289(87)	A-Type PAC DP-3 (A = 1) (a)
36b	18.06	865.1966	$C_{45}H_{38}O_{18}$	−2.2	575(42), 407(100), 289(77)	B-Type PAC DP-3
37	18.42	553.1559	$C_{25}H_{30}O_{14}$	−0.6	389(100)	unknown
38	18.67	1007.2123 (−2H)	$C_{105}H_{84}O_{42}$	−3	NA	A-Type PAC DP-7 (A = 1) (a)
39	19.33	719.1506(−2H)	$C_{75}H_{60}O_{30}$	−1.8	NA	A-Type PAC DP-5 (A = 1) (e)
40	19.93	431.0983 (−2H)	$C_{22}H_{21}O_{10}^+$	−0.2	299(100)	peonidin-3-arabinoside
41	19.99	575.1882	$C_{27}H_{32}N_2O_{12}$	−0.1	377(100)	unknown
42	20.45	1151.2441	$C_{60}H_{48}O_{24}$	−1.9	863(100), 573(77), 411(88)	A-Type PAC DP-4 (A = 1) (b)
43	20.75	720.1579 (−2H)	$C_{75}H_{62}O_{30}$	−2.7	577(16), 289(100)	B-Type PAC DP-5
44	21.1	479.0833	$C_{21}H_{20}O_{13}$	0.4	317(38), 316(100)	myricetin-3-galactoside
45	22.37	863.1816	$C_{45}H_{36}O_{18}$	−1.4	711(49), 575(100)	A-Type PAC DP-3 (A = 1) (b)
46	22.56	487.1453	$C_{21}H_{28}O_{13}$	−0.8	147(100)	unknown
47	22.73	449.0724	$C_{20}H_{18}0_{12}$	−0.3	316(100)	myricetin-3-xyloside
48	23.12	1151.2425 (−2H)	$C_{120}H_{96}O_{48}$	−4	NA	A-Type PAC DP-8 (A = 1)
49	24.03	1008.2198 (−2H)	$C_{105}H_{86}O_{42}$	−3.4	NA	B-Type PAC DP-7
50	24.65	449.0728	$C_{20}H_{18}O_{12}$	0.7	317(47), 316(100)	myricetin-3-arabinoside
51	24.97	535.1458	$C_{25}H_{28}O_{13}$	0.1	371(33), 147(81), 119(100)	coumaroyl-monotropein (a)

DOI: 10.1021/acs.jafc.8b05029
J. Agric. Food Chem. 2018, 66, 12206−12216

Table 1. continued

peak	R_t (min)	$[M - H]^-$ or $[M - 2H]^{2-}$	formula	error (ppm)	major fragment ions[a]	tentative identification[b]
52	26.2	575.1194	$C_{30}H_{24}O_{12}$	−0.1	449(100), 285(55)	A-Type PAC DP-2
53	26.32	463.0887	$C_{21}H_{20}O_{12}$	1.1	301(87), 300(100)	quercetin-3-galactoside
54	26.67	535.1453	$C_{25}H_{28}O_{13}$	−0.8	371(45), 119(100)	coumaroyl-monotropein (b)
55	26.9	577.1346	$C_{30}H_{26}O_{12}$	−1	407(100), 289(63)	B-type PAC DP-2 (c)
56	27.22	863.1819	$C_{45}H_{36}O_{18}$	−1.1	711(38), 575(100)	A-Type PAC DP-3 (A = 1) (c)
57	27.35	463.0883	$C_{21}H_{20}O_{12}$	0.3	301(76), 300(100)	quercetin-3-glucoside
58	27.62	1007.2132 (−2H)	$C_{105}H_{84}O_{42}$	−2.1	NA	A-Type PAC DP-7 (A = 1) (b)
59	27.91	493.0987	$C_{22}H_{22}O_{13}$	−0.2	331(53), 330(100), 315(18)	laricitrin-3-galactoside
60	28.6	1151.2437	$C_{60}H_{48}O_{24}$	−2.3	863(78), 575(100)	A-Type PAC DP-4 (A = 1) (c)
61	28.9	537.161	$C_{25}H_{30}O_{13}$	−0.7	373(100), 163(73), 119(70)	coumaroyl-dihydromonotropein
62	28.95	433.0776	$C_{20}H_{18}O_{11}$	−0.1	301(77), 300(100)	quercetin-3-xyloside
63	29.29	863.1822	$C_{45}H_{36}O_{18}$	−0.7	711(52), 575(100)	A-Type PAC DP-3 (A = 1) (d)
64	29.88	433.0781	$C_{20}H_{18}O_{11}$	1	301(40), 300(100)	quercetin-3-arabinopyranoside
65	30.05	719.1505 (−2H)	$C_{75}H_{60}O_{30}$	−2	575(100), 284(51)	A-Type PAC DP-5 (A = 1) (f)
66	30.57	433.078	$C_{20}H_{18}O_{11}$	0.9	301(100), 300(63)	quercetin-3-arabinofuranoside
67	32.31	447.0934	$C_{21}H_{20}O_{11}$	0.2	301(100), 300(73)	quercetin-3-rhamnoside
68	32.75	477.1043	$C_{22}H_{22}O_{12}$	0.8	315(32), 314(100)	isorhamnetin-3-galactoside
69	32.99	463.0884	$C_{21}H_{20}O_{12}$	0.5	331(100), 330(60)	laricitrin-3-pentoside
70	33.93	507.1145	$C_{23}H_{24}O_{13}$	0.1	345(100), 344(38)	syringetin-3-galactoside
71	34.09	1149.2293	$C_{60}H_{46}O_{24}$	−1.1	NA	A-Type PAC DP-4 (A = 2)
72	34.46	507.114	$C_{23}H_{24}O_{13}$	−0.8	345(100), 344(38)	syringetin-3-glucoside
73	35.76	417.0829	$C_{20}H_{18}O_{10}$	0.3	285(100), 284(70), 255(29)	kaempferol 3-pentoside
74	36.52	447.0935	$C_{21}H_{20}O_{11}$	0.6	314(100)	isorhamnetin-3-pentoside (a)
75	37.41	447.0935	$C_{21}H_{20}O_{11}$	0.6	315(23), 314(100)	isorhamnetin-3-pentoside (b)
76	37.95	447.0935	$C_{21}H_{20}O_{11}$	0.6	315(30), 314(100)	isorhamnetin-3-pentoside (c)
77	38.47	461.1092	$C_{22}H_{22}O_{11}$	0.7	314(100)	isorhamnetin-3-rhamnoside
78	38.63	477.1044	$C_{22}H_{22}O_{12}$	1.1	345(39), 344(100)	syringetin-3-pentoside
79	38.8	491.1197	$C_{23}H_{24}O_{12}$	0.7	345(100), 344(60), 313(73)	syringetin-3-rhamnoside
80	39.13	511.2186	$C_{25}H_{36}O_{11}$	0.2	163(76), 119(100)	unknown
81	39.91	609.1255	$C_{30}H_{26}O_{14}$	0.9	463(95), 300(100)	quercetin-3-*O*-(6″-p-coumaroyl)-*β*-galactoside
82	41.02	567.1145	$C_{28}H_{24}O_{13}$	0.2	301(100), 300(64)	quercetin-3-*O*-(6″-benzoyl)-*β*-galactoside

[a]NA: not available. [b]Abbreviations: PAC, proanthocyanidin; DP, degree-of-polymerization; A, number of A-type linkages.

Benzoic Acid, Hydroxybenzoic Acid, and Their Derivatives. Peak 1 had an $[M - H]^-$ ion at m/z 167.0346, suggesting that its formula is $C_8H_8O_4$ (−2.1 ppm). Its major fragment ions were m/z 152 and 108, indicating successive losses of CH_3 (167 → 152) and COO (152 → 108) units. The molecular and fragment ions are consistent with previous report on vanillic acid.[17] Peak 2 had an $[M - H]^-$ ion at m/z 299.0769 ($C_{13}H_{16}O_8$, −1.1 ppm) and the main fragment ions at m/z 179, 137, and 93. These ions suggest losses of the hexose moiety ($C_6H_{10}O_5$, 162 Da) and COO (44 Da) group during fragmentation; thus, the compound was putatively identified as hydroxybenzoic acid glucoside.[18] Peak 20 with an $[M - H]^-$ ion at m/z 121.0294 ($C_7H_6O_2$, −0.9 ppm) was identified as benzoic acid by loss of its COO unit during fragmentation (m/z 77) and characteristic UV absorbance bands in the 200, 230, and 280 nm regions.[19] Vanillic acid, benzoic acid, and hydroxybenzoic acids are known phenolic acids in the cranberry fruit.[13,20]

Peaks 13, 22, 23, and 27 all share strong fragment ion of m/z 121 ($C_7H_5O_2$), suggesting one benzoyl group in their structures, which was also confirmed by their similar UV absorbance spectra in comparison to that of benzoic acid. On the basis of their neutral loss of 324 Da (2 × hexose, peaks 13 and 23), 340 Da (2 × hexose + hydroxy group, peak 22) and 294 Da (hexose + pentose, peak 27), they were putatively identified as benzoyl-hexosyl-hexoside ($C_{19}H_{26}O_{12}$, peaks 13 and 23), hydroxybenzoyl-hexosyl-hexoside ($C_{19}H_{26}O_{13}$, peak 22), and benzoyl-pentosyl-hexoside ($C_{18}H_{24}O_{11}$, peak 27). Peak 33 had a molecular ion at m/z 371.0985 ($C_{16}H_{20}O_{10}$, 0.2 ppm) and a fragment ion at m/z 249. The neutral loss of 122 Da corresponds to benzoic acid. It was putatively identified as 3-(benzoyloxy)-2-hydroxypropyl glucopyranosiduronic acid.

Hydroxycinnamic Acid and Its Derivatives. Peaks 8 and 16 showed identical $[M - H]^-$ ions at m/z 163.0398 ($C_9H_8O_3$, −1.8 ppm) and a fragment ion at m/z 119. The loss of 44 Da unit indicates a COO unit, and the compound formula and fragments are consistent with coumaric acid.[17] Thus, the two peaks were putatively identified as coumaric acid isomers. Peak 18 had $[M - H]^-$ ion at m/z 353.0875 ($C_{18}H_{18}O_9$, −0.7 ppm) and a fragment ion at m/z 191 ($C_7H_{11}O_6$). Its formula is consistent with chlorogenic acid (caffeoylquinic acid), and the fragment corresponds to the quinic acid ion that resulted from the cleavage of the ester bond.[21] Peak 24 had an $[M - H]^-$ ion at m/z 223.0609 ($C_{11}H_{12}O_5$, −1.2 ppm). Its fragment ions were at m/z 208, 164, and 149, suggesting two CH_3 (15 Da) groups and one COO (44 Da) group in its structure. Such a fragmentation pattern and structural details are consistent with sinapic acid.[22]

DOI: 10.1021/acs.jafc.8b05029
J. Agric. Food Chem. 2018, 66, 12206−12216

Peaks 7 and 14 exhibited the same molecular ions (m/z 341.0875, $C_{15}H_{18}O_9$) but different fragmentation patterns. Peak 7 had a strong fragment ion at m/z 161 and others at m/z 179 and 133. Peak 14 only gave two fragment ions at m/z 179 and 135. The molecular and fragment ions of peak 14 match exactly with caffeic acid glucoside, reported by Jaiswal et al.[23] During fragmentation the glycosidic bond was cleaved, resulting in ions of caffeic acid (m/z 179) and its fragment (−COO, m/z 135). Ions of peak 7 are partially in agreement with one of the caffeoyl-glucose (ester) isomers,[23] as they both produced strong fragment ions at m/z 161. Thus, the two molecules were putatively identified as caffeoyl-glucose (peak 7) and caffeic acid glucoside (peak 14). Using the same strategy, peak 5 (m/z 325.0926, $C_{15}H_{18}O_8$) was assigned as coumaric acid glucoside for its fragment ions of m/z 163 and 119 (same fragment ions of coumaric acid).[17] Peaks 17 and 21 with the same $[M - H]^-$ ions at m/z 325 were assigned as isomers of coumaroyl-glucose, from their fragment ions at m/z 145. Similarly, peaks 26 and 30a were identified as feruloyl-glucose and sinapoyl-glucose, respectively. Peak 6 with an $[M - H]^-$ ion at m/z 503.1410 ($C_{21}H_{28}O_{14}$, 0.6 ppm) exhibited successive losses of two 162 Da units and was identified as glucosyl-caffeoyl-glucose. Similarly identified hydroxycinnamic acid derivatives have been previously found in cranberry.[24]

Peaks 51 and 54 share the same $[M - H]^-$ ion ($C_{25}H_{28}O_{13}$) and similar fragmentation patterns. The m/z 371 fragment ($C_{16}H_{19}O_{10}$) corresponds to monotropein, and the m/z 119 fragment suggests a structure of coumaric acid. Thus, they were putatively identified as coumaroyl-monotropeins.[25] Peak 61 had two additional hydrogens in both the molecular and fragment ions in comparison to the two monotropeins; therefore, it was identified as coumaroyl-dihydromonotropein. These compounds have been reported in previous studies on cranberry.[25,26]

Flavonol Glycosides. The fragmentation pattern of flavonol glycosides is characterized by homolytic and heterolytic cleavage of their glycosidic bonds, resulting in radical and nonradical aglycone ions.[27] Typical neutral losses in flavonol glycoside fragmentation include 132/133 Da (pentose), 146/147 Da (deoxyhexose), and 162/163 Da (hexose) or their combinations in the case of multiple glycosylation. In the study, peaks 44, 47, and 50 share fragment ions at m/z 316 ($C_{15}H_8O_8$) and 317 ($C_{15}H_9O_8$), which correspond to myricetin aglycone ions. Their neutral losses suggest a hexose (peak 44) or pentose (peaks 47, 50) moiety, and they were putatively identified as myricetin-3-galactoside (peak 44), myricetin-3-xyloside (peak 47), and myricetin-3-arabinoside (peak 50), which have been reported in a previous study.[28]

Peaks 53, 57, 62, 64, 66, 67, 81, and 82 share common fragment ions at m/z 300 ($C_{15}H_8O_7$) and 301 ($C_{15}H_9O_7$), indicating that they are quercetin glycosides. Peaks 53 and 57 had neural losses of 162/163 Da, suggesting that they are quercetin hexosides. The high intensity of peak 53 suggests that it is quercetin-3-galactoside, the most abundant flavonol glycoside in cranberry.[13] Accordingly, peak 57 was identified as quercetin-3-glucoside. Peaks 62, 64, and 66 share neutral losses of 132/133 Da, indicating that they are quercetin pentosides. They were respectively identified as quercetin-3-xyloside, quercetin-3-arabinopyranoside, and quercetin-3-arabinofuranoside on the basis of prior publications.[13,28] Similarly, peak 67 was identified as quercetin-3-rhamnoside by its neutral loss of 146/147 Da. Peak 81 (m/z 609.1255, $C_{30}H_{26}O_{14}$, 0.9 ppm) had fragment ions of m/z 463 and 300, indicating that it is a quercetin hexoside derivative. The loss of 146 Da suggests the coumaroyl group. It was identified as quercetin-3-*O*-(6″-p-coumaroyl)-β-galactoside. Correspondingly, peak 82 was assigned as quercetin-3-*O*-(6′′-benzoyl)-β-galactoside. These two derivatives have been previously characterized in cranberry powder.[28]

Other flavonol peaks showing characteristic neutral losses of sugar moieties had fragment ions at m/z 244/285, 314/315, 330/331, and 344/345. These are characteristic ions of kaempferol, isorhamnetin (methylquercetin), laricitrin (methylmyricetin), and syringetin (dimethylmyricetin) aglycones. Accordingly, these peaks were identified as glycosides (galactoside, glucoside, pentoside, or rhamnoside) of such aglycones.

Proanthocyanidins. Peaks 12 and 29 had the same $[M - H]^-$ ion at m/z 289.071 ($C_{15}H_{14}O_6$) and fragment ions at m/z 245 and 203. They were identified as catechin and epicatechin after the matching of molecular ion, fragment ions, and retention times with reference standards. Proanthocyanidin oligomers and polymers were identified by their characteristic $[M - H]^-$ and/or $[M - 2H]^{2-}$ ions, such as m/z 575−577 (dimers), 861−865 (trimers), 1147−1153 (tetramers), 718−720 ($[M - 2H]^{2-}$) and 1435−1441 (pentamers), 861−864 ($[M - 2H]^{2-}$, hexamers), 1005−1008 ($[M - 2H]^{2-}$, heptamers), and 1150−1152 ($[M - 2H]^{2-}$, heptamers). Doubly charged ions were determined by their different distances between isotopes (~0.50 Da) in comparison to ~1 Da of singly charged ions.[29] The presence and number of A-type interflavan linkages were determined by the loss of two hydrogens per linkage (due to the formation of C−O−C bonds) in comparison to B-type molecules. A total of 20 A-type proanthocyanidins were identified.

Although cranberry is well-known for its rich profile of A-type proanthocyanidins,[30] herein we also detected several B-type proanthocyanidin oligomers, such as dimers (peaks 10, 25, 55), trimer (peak 36b), tetramer (peak 32), pentamer (peak 43), and heptamer (peak 49), which indicates a comprehensive proanthocyanidin profile in cranberry.

Other Compounds. Peak 3 had a $[M - H]^-$ ion at m/z 315.1081 ($C_{14}H_{20}O_8$, −1.3 ppm) and fragment ions at m/z 153 and 123. The losses of 162 and 40 Da units indicate a hexose moiety and a CH_2O group in this molecule. Such a fragmentation pattern is consistent with a previous report on hydroxytyrosol glucoside.[31] Peak 35 showed two molecular ions at m/z 461.1092 and 479.1194 and fragment ions at m/z 299 and 298. It exhibited a 520 nm absorbance peak, which is characteristic of anthocyanins. It was identified as peonidin-3-galactoside ($C_{22}H_{23}O_{11}^+$), one of the major reported cranberry anthocyanins.[32] The m/z 461 and 479 ions correspond to its $[M^+ - 2H]^-$ and $[M^+ - 2H + H_2O]^-$ adducts, which are typically formed from anthocyanin cations under negative ionization.[33] Similarly, peak 40 with an $[M - 2H]^-$ ion at m/z 431.0983 ($C_{22}H_{23}O_{11}^+$, −0.2 ppm) and a fragment ion at m/z 299 was tentatively identified as peonidin-3-arabinoside.

Isomeric Ions in Cranberries. Isomeric ions are defined as the ions sharing same accurate mass and molecular formula. A few isomers were found among identified cranberry metabolites, including both stereoisomers (i.e., coumaric acid isomers, catechin, and epicatechin) and structural isomers (i.e., different flavonol hexosides or pentosides). For most isomeric ions, UPLC provided sufficient separation to differentiate between them. However, some isomeric ions were not resolved chromatographically and thus they could not be differentiated with conventional mass spectrometric detection. In the current

DOI: 10.1021/acs.jafc.8b05029
J. Agric. Food Chem. 2018, 66, 12206−12216

Table 2. List of Coeluted Isomeric Ions Discriminated by Ion Mobility[a]

m/z	R_t (min)	CCS (Å^2)	detector count	identification
163.0397–163.0398	7.28	168.84	4827	coumaric acid isomers
		197.68	12404	
	9.82	168.9	18299	
		198.45	4372	
191.0557–191.0559	13.40	133.59	1793	$C_7H_{12}O_6$
		174.1	4088	
	15.13	170.44	2174	
		192.85	6748	
		133.37	3759	
	18.08	133.68	3625	
		194.09	2522	
		171.65	6360	
223.0609	12.29	182.8	4140	sinapic acid isomers
		207.75	13178	
271.0609	30.09	162.1	4617	$C_{15}H_{12}O_5$
		187.4	15668	
289.0714	14.00	158.25	335069	epicatechin isomers
		224.34	13900	
315.1081	5.04	244.31	3977	hydroxytyrosol glucoside isomers
		174.86	22604	
325.0927–325.0928	10.18	209.87	18048	coumaroyl-glucose isomers
		182.22	180817	
		265.7	7197	
		237.3	4983	
	11.11	182.11	37289	
		210.16	3100	
353.0875	10.38	177.61	35686	chlorogenic acid iosmers
		255.58	3130	
415.1246	13.16	206.47	642729	benzoyl-pentosyl-hexoside isomers
		277.91	12472	
425.0875	12.76	193.58	5628	$C_{22}H_{18}O_9$
		223.84	46052	
433.0776–433.0780	28.96–29.01	295.85	2549	quercetin-pentoside isomers
		268.35	3505	
		199.14[b]	377800	
	30.63	198.89[c]	805559	
		253.67	12338	
447.0934	32.37	285.04	2389	quercetin-3-rhamnoside isomers
		197.47	515276	
449.0728	24.71	266.62	4436	myricetin-3-arabinoside isomers
		200.47	497215	
463.0887	26.32–26.41	141.96	2111	quercetin-hexoside isomers
		201.98[d]	3058183	
		413.81	4569	
		373.09	3400	
		475.29	4761	
		335	4621	
		542.66	3264	
		311.9	6860	
		271.33	131898	
		166.85	5522	
479.0833	21.14	204.33[e]	1289458	myricetin-hexoside isomers
		275.58	27946	
575.1194–575.1196	26.23–26.27	294.66	1814	A-type PAC DP-2 isomers
		179.71	28140	
		231.21	517976	
	29.33–29.36	178.77	16166	
		229.21	1741	
863.1813–863.1820	13.76–13.79	281.35	5231	A-type PAC DP-3 isomers
		220.29	7994	
	14.83–14.85	264.53	2578	
		218.1	7606	
	22.43–22.45	278.53	426542	
		217.83	22631	
	27.30	278.72	289946	
		218.51	10278	
1151.2444–1151.2455	17.08–17.14	252.33	3557	A-type PAC DP-4 isomers
		337.4	8754	
	28.94–28.96	214.39	3653	
		330.56	72459	

[a]CCS values and detector counts were extracted from one representative cranberry sample. [b]Quercetin-3-xyloside. [c]Quercetin-3-arabinofuranoside. [d]Quercetin-3-galactoside. [e]Myricetin-3-galactoside.

study, the addition of ion mobility detection provided an extra dimension of ion separation, enabling differentiation of coeluting isomeric ions.

Some examples of coeluted isomers discriminated by their different collisional cross-section (CCS, representing ion mobility) values are reported in Table 2. Some chromatographically separated structural isomers, i.e., some coumaric acid derivatives, epicatechins, coumaroyl-hexoses, and proanthocyanidin oligomers, were found to consist of multiple stereoisomers with the same retention times. Among these chromatographically nonresolved isomeric ions, usually there is a dominant ion (main component) with the other ions at much lower intensities. The existence of these isomers indicates a very complicated metabolomic profile for cranberry. The resolving power of ion mobility for isomers has great potential in the analysis of biomolecules containing extensive isomeric forms, such as proanthocyanidins.

Chemometric Analysis of Metabolomic Profiles of Different Cranberry Cultivars. Chemometric methods were used to compare the metabolomic profiles of the 10 cranberry cultivars. The UPLC-HRMS data acquired were first processed by Progenesis QI, and a total of 4778 ion ions were detected. They were exported into a two-dimensional 80 × 4778 (samples × mass peaks) matrix in Excel. Pareto data scaling was conducted prior to analysis to avoid emphasis on peaks with high intensities and reduce the effect of artifacts and noise.[15]

Both PCA and OPLS-DA were applied on the MS data matrix and revealed the same sample clustering pattern (Figure 2A; PCA data not shown). As an unsupervised model, PCA can be affected by experimental variations unrelated to samples, such as instrument drift and system noise,[15] making the supervised model OPLS-DA a better choice. In comparison to PLS-DA, the OPLS-DA model is rotated so that different

DOI: 10.1021/acs.jafc.8b05029
J. Agric. Food Chem. 2018, 66, 12206–12216

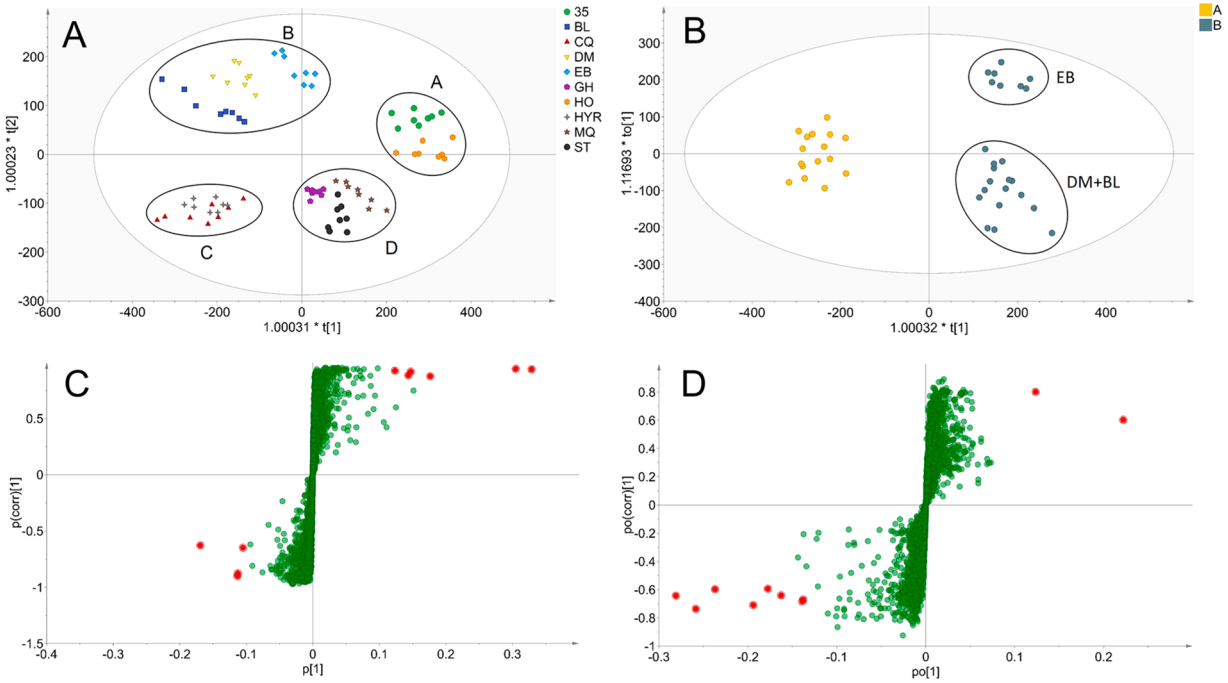

Figure 2. OPLS-DA on the UPLC-HRMS profiles of cranberry cultivars: (A) score plot on the first two predictive components of 10 cranberry cultivars; (B) score plot for model on cultivar group A vs B; (C) S-plot for predictive component from model A vs B; (D) S-plot for orthogonal component from model A vs B. Important variables are marked in red and given in Table 3.

classes are separated at predictive component (t_p), whereas variation unrelated to class separation is found in orthogonal components (t_o).[15] With such component separation, the OPLS-DA model can be better interpreted.

In the OPLS-DA score plot consisting of 10 cultivars (Figure 2A), different cranberry samples can be associated into four groupings with each consisting of two to three cultivars. Group A contains 35 and HO, group B consists of EB, DM, and BL, group C contains HYR and CQ, and group D comprises MQ, ST, and GH. The grouping of certain cranberry cultivars suggests similar metabolomic profiles that generally reflect their ancestry (Figure 1). HO and its progeny 35 tightly clustered to form group A. DM is the progeny of both BL and EB, and the three cultivars loosely formed group B with DM in the middle. CQ and HYR were hybrids separately developed by Rutgers University (NJ) and the University of Wisconsin—Madison (WI) and share ancestry derived from ST and BL, forming group C as one tight cluster. ST and GH have the common parent "McFarlin", and MQ and GH have a common grandparent, Searles. These three cultivars formed group D.

MQ as the progeny of 35 did not fall in same group with 35 and HO. 35 has 50% genes in common with HO (the other parent being Searles). MQ, being the second-generation offspring of HO, is only 25% genetically in common with HO. If the metabolomic profile of group A is a result of the HO genetic background, then HO and 35 would be more similar. Also, the other parent of MQ is the cultivar Lemunyon (not included in this study), which contributed 50% genetically to MQ and may have a significant influence metabolically.

On the basis of the cultivar clustering information, another series of OPLS-DA was then carried out on different pairs (six in total) of cultivar groups identified in the score plot. Figure 2B is the OPLS-DA score plot of group A and group B cultivars. In the plot, the two groups were separated on the predictive component (x axis), which contributes to between-class variation. A subgroup separation was also observed in group B, in which the EB samples were separated from DM and BL on the orthogonal component (y axis) that contributes to within-class variation. Such separation can be explained by DM's sharing 50% genetic background with BL whereas only 25% background is shared with EB (Figure 1).

Two S-plots were generated for predictive and orthogonal components in this OPLS-DA model (Figure 2C,D). They visualize the variable influence through combination of covariance and correlation loading profiles. Variables that strongly contribute to between- or within-class separation are located at the top right and bottom left of S-plots, with both high covariance and correlation loadings.[15] On the basis of such criteria, important compounds with considerable variation were determined. The same analyses were applied to other pairs of cranberry cultivar groups, and their corresponding OPLS-DA score plots and S-plots can be found in Figure S2 (Supporting Information). A list of important compounds is summarized in Table 3. They were identified by the associated retention time and accurate mass data, together with their fragmentation spectra retrieved from MS chromatograms.

Six variables having greater variation in most of the predictive components in different models appeared to be anthocyanins. They consist of galactosides and arabinosides of peonidin or cyanidin, which are the major anthocyanin components in cranberry.[32] On the basis of the variable distribution of the S-plots, anthocyanin levels in different cultivar groups should be A < D < B/C, which is confirmed by the average anthocyanin peak intensity shown in Figure 3A–D. Anthocyanins as pigment compounds account for the red fruit color, which has been the major focus in cranberry breeding. Some of the cultivars analyzed in the current study were also included in previous publications and exhibited similar variation on individual or total anthocyanin contents.[13,14]

DOI: 10.1021/acs.jafc.8b05029
J. Agric. Food Chem. 2018, 66, 12206−12216

Table 3. Important Cranberry Metabolites Identified by S-Plots on Different OPLS-DA Models

variable ID (R_t_m/z)	OPLS-DA S-plot[a] A–B	A–C	A–D	B–C	B–D	C–D	A–B ortho	identity	class
13.19_465.1037	T	T	T		B	B		cyanidin-3-galactoside (+H_2O)	anthocyanin
15.82_417.0825	T	T			B	B		cyanidin-3-arabinoside	
17.39_461.1090	T	T	T	T	B	B		peonidin-3-galactoside	
17.39_479.1194	T	T	T	T	B	B		peonidin-3-galactoside (+H_2O)	
20.08_449.1089	T	T			B	B		peonidin-3-arabinoside (+H_2O)	
20.10_431.0983	T	T	T		B	B		peonidin-3-arabinoside	
20.49_479.1193						B		methoxykaempferol-hexoside	flavonol
21.18_479.0833	B				T			myricetin-3-galactoside	
24.77_449.0727	B							myricetin-3-arabinoside	
26.42_927.1822							B	quercetin-3-galactoside (dimer)	
26.43_464.0915							B	quercetin-3-galactoside (isotopic)	
29.05_433.0777							B	quercetin-3-xyloside	
30.68_433.0778							B	quercetin-3-arabinofuranoside	
32.40_447.0934						T	T	quercetin-3-rhamnoside	
34.05_507.1142				T			B	syringetin-3-galactoside	
37.50_447.0934		T	T	T		B		isorhamnetin-3-pentoside (b)	
38.03_447.0935		T		T		B	B	isorhamnetin-3-pentoside (c)	
41.08_567.1141				B	B			quercetin-3-O-(6″-benzoyl)-β-galactoside	
11.56_431.1560			B	B	B		B	benzyl-hexosyl-hexoside (isomer)	benzoyl/benzyl derivative
15.72_371.0982							B	3-(benzoyloxy)-2-hydroxypropyl glucopyranosiduronic acid	
10.20_325.0926		T	T	T				coumaroyl-glucose (a)	coumaric acid derivative
25.06_535.1454				B	B			coumaroyl-monotropein (a)	
26.74_535.1454		B	B	B	B			coumaroyl-monotropein (b)	
27.22_537.1607			B	B	B			coumaroyl-dihydromonotropein (isomer)	
28.95_537.1611		B	B	B	B			coumaroyl-dihydromonotropein	
29.02_575.1189	B	B	B					A-type DP-4 (A = 1) (isomer)	proanthocyanidin
29.38_863.1815	B	B	B					A-type DP-3 (A = 1) (d)	
10.27_481.1463							T	$C_{21}H_{26}N_2O_{11}$	unknown
20.02_575.1880		T	T			B		$C_{27}H_{32}N_2O_{12}$	
22.10_577.2035						B		$C_{27}H_{34}N_2O_{12}$	

[a]Abbreviations: T, top of the plot; B, bottom of the plot; ortho, orthogonal component.

Several flavonol glycosides also exhibited strong variation among cultivars. The most notable one is the appearance of quercetin glycosides in the S-plot of orthogonal component in model A–B (Figure 2D), indicating their differential levels between EB and DM/BL. For instance, EB had a considerably higher level of quercetin-3-rhamnoside in comparison to DM and BL and lower levels of quercetin-3-galactoside/arabinoside (Figure 3E–G). In addition, different cultivar groups had considerable variation on the two isorhamnetin-3-pentosides (Figure 3H).

Two benzoyl/benzyl derivatives—a newly identified benzyl-hexosyl-hexoside isomer and 3-(benzoyloxy)-2-hydroxypropyl glucopyranosiduronic acid—also contributed to the within-class variation of group B (EB vs DM/BL). In Figure 3I–J, EB contained lower levels of the two compounds in comparison to DM and BL. In addition, the benzyl-hexosyl-hexoside isomer also appeared as an important variable in the S-plots of models A–D, B–C, and B–D, indicating it varied in concentration among these cultivar groups. In Figure 3K, this compound exhibited the highest concentration in group B and low concentrations in groups C and D.

Five coumaric acid derivatives were identified to contribute to the variations across different cultivars. Among them, four coumaroyl iridoids including two coumaroyl-monotropein isomers and two coumaroyl-dimonotropein isomers had significantly higher concentrations in groups A and B than in groups C and D (Figure 3L,M). In contrast, the coumaroyl-glucose (a) exhibited an opposite concentration pattern in the cultivar groups, with higher concentrations in groups C and D (Figure 3N). The biosynthesis of such molecules involves coumaric acid as a common substrate. Their negative correlation patterns suggest that coumaric acids have been preferably channeled to different biosynthetic pathways in certain cranberry cultivars, potentially due to differential enzyme activities.

Two A-type proanthocyanidin oligomers, one trimer and one tetramer, exhibited strong cross-cultivar variations. In Figure 3O,P, they had the highest concentrations in group A, followed by group D, and were produced in much lower levels in groups B and C. It should be noted that cultivars in groups B and C contained the highest levels of anthocyanins (Figure 3A–D). Such oppositing concentration patterns between proanthocyanidins and anthocyanins suggests diverted resource partitioning in the flavonoid biosynthetic pathway of different cranberry cultivars. Similar observations were reported in previous studies on cranberry.[11−13]

OPLS-DA and other multivariate data analyses such as principal component analysis (PCA) have been successfully used in the evaluation, modeling, and visualization of different forms of data complexes, acquired from GC-MS,[15,34] LC-

DOI: 10.1021/acs.jafc.8b05029
J. Agric. Food Chem. 2018, 66, 12206−12216

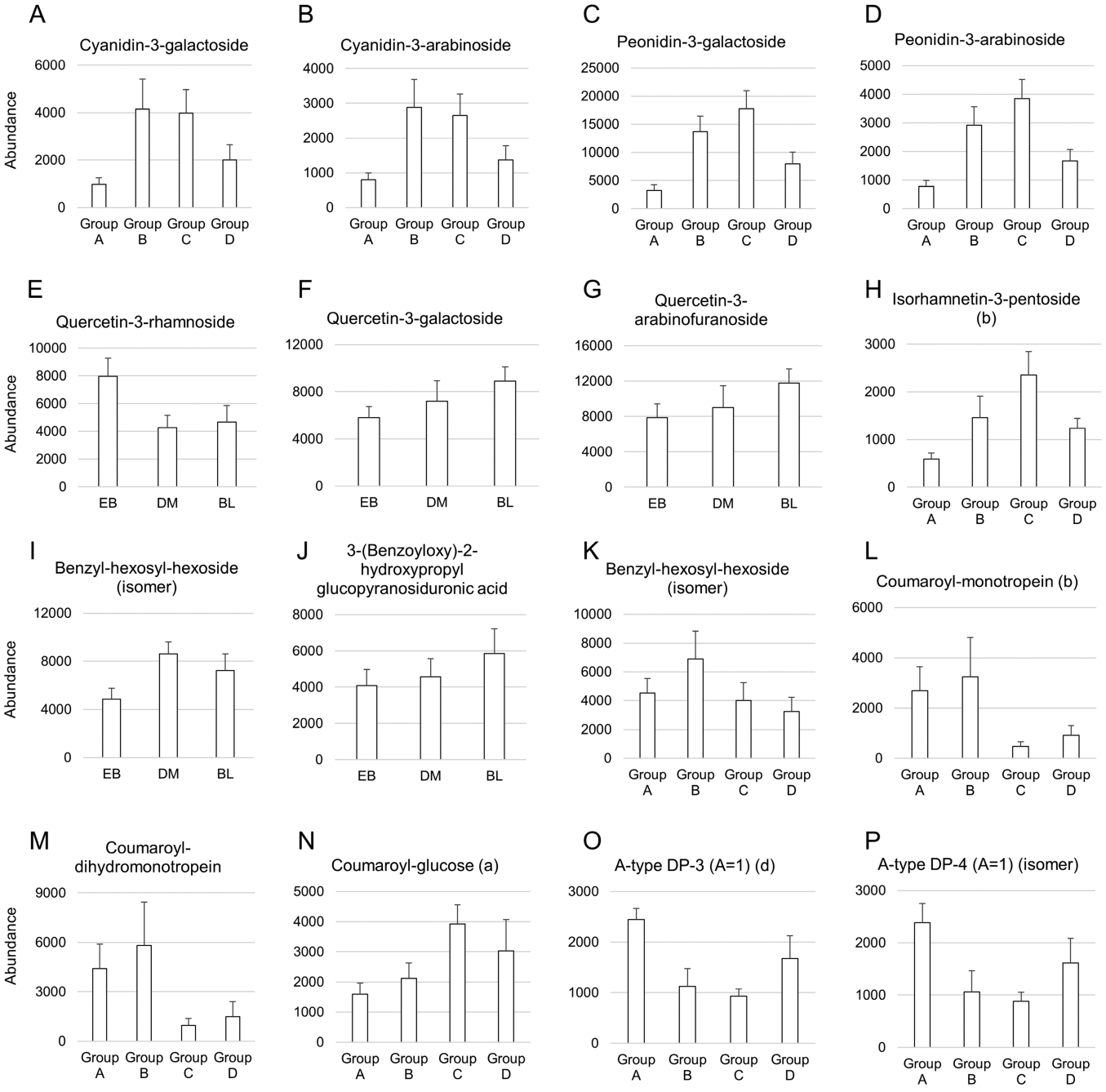

Figure 3. Average ion abundance of important cranberry metabolites identified by OPLS-DA.

MS,[35,36] NMR[37,38] and other spectroscopic analyses (UV, NIR, MIR).[37,39] Their application in the current study provided robust and efficient data interpretation on the cranberry metabolomic profiles. Cultivar clustering was apparent and clearly related with their genetic backgrounds. Over 30 important compounds were determined, belonging to the major cranberry phytochemical groups. These findings can be used to guide future targeted analysis on selected components.

Cranberry phytochemicals continue to receive much research interest as they relate to nutritional values and potential human health benefits. In this study, a comprehensive metabolomic profile consisting of over 80 components was identified through UPLC-IM-HRMS, covering major documented cranberry phenolic classes such as phenolic acids, anthocyanins, flavonols, and proanthocyanidins. Analysis of an HRMS data matrix using OPLS-DA revealed both metabolomic similarities and differences among cranberry cultivars and identified specific phenolic compounds having strong cross-cultivar variations. This study further expanded our knowledge on the cranberry phenolic compound composition, adding critical information on the evaluation of cranberry's potential health benefits. The phenolic variation among different cultivars can be used as a valuable guide for future cranberry breeding practice focusing on phenolic compound improvement. The nontargeted metabolomic approach has great value for future studies in phytochemical analysis of cranberry or other agricultural products and can be extremely efficient in large complex data sets.

DOI: 10.1021/acs.jafc.8b05029
J. Agric. Food Chem. 2018, 66, 12206−12216

■ ASSOCIATED CONTENT

Supporting Information

The Supporting Information is available free of charge on the ACS Publications website at DOI: 10.1021/acs.jafc.8b05029.

UPLC chromatograms of cranberry extract, score plots, and S-plots of OPLS-DA models on different cranberry cultivar groups (PDF)

■ AUTHOR INFORMATION

Corresponding Author

*P.C.: e-mail, pei.chen@ars.usda.gov; tel, +1 301 504 8144; fax, +1 301 504 8314.

ORCID

Peter de B. Harrington: 0000-0003-0268-8630

Pei Chen: 0000-0002-1457-5177

Funding

This study was supported by the Agricultural Research Service of the U.S. Department of Agriculture and an Interagency Agreement with the Office of Dietary Supplements of the National Institute of Health.

Notes

The authors declare no competing financial interest.

■ REFERENCES

(1) Polashock, J.; Zelzion, E.; Fajardo, D.; Zalapa, J.; Georgi, L.; Bhattacharya, D.; Vorsa, N. The American cranberry: First insights into the whole genome of a species adapted to bog habitat. *BMC Plant Biol.* **2014**, *14*, 165.

(2) Pappas, E.; Schaich, K. M. Phytochemicals of cranberries and cranberry products: Characterization, potential health effects, and processing stability. *Crit. Rev. Food Sci. Nutr.* **2009**, *49*, 741−781.

(3) Blumberg, J. B.; Camesano, T. A.; Cassidy, A.; Kris-Etherton, P.; Howell, A.; Manach, C.; Ostertag, L. M.; Sies, H.; Skulas-Ray, A.; Vita, J. A. Cranberries and Their Bioactive Constituents in Human Health. *Adv. Nutr.* **2013**, *4*, 618−632.

(4) Shukitt-Hale, B.; Galli, R. L.; Meterko, V.; Carey, A.; Bielinski, D. F.; McGhie, T.; Joseph, J. A. Dietary supplementation with fruit polyphenolics ameliorates age-related deficits in behavior and neuronal markers of inflammation and oxidative stress. *Age (Omaha).* **2005**, *27*, 49−57.

(5) Neto, C. C. Cranberry and its phytochemicals: a review of in vitro anticancer studies. *J. Nutr.* **2007**, *137*, 186S−193S.

(6) Hancock, J. F.; Lyrene, P.; Finn, C. E.; Vorsa, N.; Lobos, G. A. Blueberries and cranberries. In *Temperate Fruit Crop Breeding: Germplasm to Genomics*; Hancock, J. F., Ed.; Springer Science + Business Media: Berlin, Germany, 2008; pp 115−149.

(7) Chandler, F. B.; Wilcox, R. B.; Bain, H. F.; Bergman, H. F.; Dermen, H. Cranberry breeding investigation of the US Dept. of Agriculture. *Cranberries* **1947**, *12*, 6−9.

(8) Roper, T. R. 'Steven'cranberry. *J. Am. Pomol. Soc.* **2001**, *55*, 66.

(9) McCown, B. H.; Zeldin, E. L. HyRed", an early, high fruit color cranberry hybrid. *HortScience* **2003**, *38*, 304−305.

(10) Wink, M. Plant breeding: importance of plant secondary metabolites for protection against pathogens and herbivores. *Theor. Appl. Genet.* **1988**, *75*, 225−233.

(11) Vvedenskaya, I. O.; Vorsa, N. Flavonoid composition over fruit development and maturation in American cranberry, *Vaccinium macrocarpon* Ait. *Plant Sci.* **2004**, *167*, 1043−1054.

(12) Carpenter, J. L.; Caruso, F. L.; Tata, A.; Vorsa, N.; Neto, C. C. Variation in proanthocyanidin content and composition among commonly grown North American cranberry cultivars (*Vaccinium macrocarpon*). *J. Sci. Food Agric.* **2014**, *94*, 2738−2745.

(13) Wang, Y.; Johnson-Cicalese, J.; Singh, A. P.; Vorsa, N. Characterization and quantification of flavonoids and organic acids over fruit development in American cranberry (*Vaccinium macrocarpon*) cultivars using HPLC and APCI-MS/MS. *Plant Sci.* **2017**, *262*, 91−102.

(14) Brown, P. N.; Murch, S. J.; Shipley, P. Phytochemical diversity of cranberry (*Vaccinium macrocarpon* Aiton) cultivars by anthocyanin determination and metabolomic profiling with chemometric analysis. *J. Agric. Food Chem.* **2012**, *60*, 261−271.

(15) Wiklund, S.; Johansson, E.; Sjöström, L.; Mellerowicz, E. J.; Edlund, U.; Shockcor, J. P.; Gottfries, J.; Moritz, T.; Trygg, J. Visualization of GC/TOF-MS-based metabolomics data for identification of biochemically interesting compounds using OPLS class models. *Anal. Chem.* **2008**, *80*, 115−122.

(16) Lin, L. Z.; Harnly, J.; Zhang, R. W.; Fan, X. E.; Chen, H. J. Quantitation of the hydroxycinnamic acid derivatives and the glycosides of flavonols and flavones by UV absorbance after identification by LC-MS. *J. Agric. Food Chem.* **2012**, *60*, 544−553.

(17) Fang, N.; Yu, S.; Prior, R. L. LC/MS/MS characterization of phenolic constituents in dried plums. *J. Agric. Food Chem.* **2002**, *50*, 3579−3585.

(18) Álvarez-Fernández, M. A.; Cerezo, A. B.; Cañete-Rodríguez, A. M.; Troncoso, A. M.; García-Parrilla, M. C. Composition of nonanthocyanin polyphenols in alcoholic-fermented strawberry products using LC-MS (QTRAP), high-resolution MS (UHPLC-Orbitrap-MS), LC-DAD, and antioxidant activity. *J. Agric. Food Chem.* **2015**, *63*, 2041−2051.

(19) Saad, B.; Bari, M. F.; Saleh, M. I.; Ahmad, K.; Talib, M. K. M. Simultaneous determination of preservatives (benzoic acid, sorbic acid, methylparaben and propylparaben) in food stuffs using high-performance liquid chromatography. *J. Chromatogr. A* **2005**, *1073*, 393−397.

(20) Zuo, Y.; Wang, C.; Zhan, J. Separation, characterization, and quantitation of benzoic and phenolic antioxidants in American cranberry fruit by GC-MS. *J. Agric. Food Chem.* **2002**, *50*, 3789−3794.

(21) Clifford, M. N.; Johnston, K. L.; Knight, S.; Kuhnert, N. Hierarchical scheme for LC-MSn identification of chlorogenic acids. *J. Agric. Food Chem.* **2003**, *51*, 2900−2911.

(22) Engels, C.; Schieber, A.; Ganzle, M. G. Sinapic acid derivatives in defatted Oriental mustard (*Brassica juncea* L.) seed meal extracts using UHPLC-DAD-ESI-MSn and identification of compounds with antibacterial activity. *Eur. Food Res. Technol.* **2012**, *234*, 535−542.

(23) Jaiswal, R.; Matei, M. F.; Glembockyte, V.; Patras, M. A.; Kuhnert, N. Hierarchical key for the LC-MSn identification of all ten regio- and stereoisomers of caffeoylglucose. *J. Agric. Food Chem.* **2014**, *62*, 9252−9265.

(24) Marwan, A. G.; Nagel, C. W. Identification of the hydroxycinnamtic acid derivatives in cranberries. *J. Food Sci.* **1982**, *47*, 774−778.

(25) Jensen, H. D.; Krogfelt, K. A.; Cornett, C.; Hansen, S. H.; Christensen, S. B. Hydrophilic Carboxylic Acids and Iridoid Glycosides in the Juice of American and European Cranberries (*Vaccinium macrocarpon* and *V. oxycoccos*), Lingonberries (*V. vitis-idaea*), and Blueberries (*V. myrtillus*). *J. Agric. Food Chem.* **2002**, *50*, 6871−6874.

(26) Turner, A.; Chen, S. N.; Nikolic, D.; Van Breemen, R.; Farnsworth, N. R.; Pauli, G. F. Coumaroyl iridoids and a depside from cranberry (*Vaccinium macrocarpon*). *J. Nat. Prod.* **2007**, *70*, 253−258.

(27) Hvattum, E.; Ekeberg, D. Study of the collision-induced radical cleavage of flavonoid glycosides using negative electrospray ionization tandem quadrupole mass spectrometry. *J. Mass Spectrom.* **2003**, *38*, 43−49.

(28) Vvedenskaya, I. O.; Rosen, R. T.; Guido, J. E.; Russell, D. J.; Mills, K. A.; Vorsa, N. Characterization of Flavonols in Cranberry (*Vaccinium macrocarpon*) Powder. *J. Agric. Food Chem.* **2004**, *52*, 188−195.

(29) Lin, L. Z.; Sun, J.; Chen, P.; Monagas, M. J.; Harnly, J. M. UHPLC-PDA-ESI/HRMSn profiling method to identify and quantify oligomeric proanthocyanidins in plant products. *J. Agric. Food Chem.* **2014**, *62*, 9387−9400.

(30) Neto, C. C.; Krueger, C. G.; Lamoureaux, T. L.; Kondo, M.; Vaisberg, A. J.; Hurta, R. A. R.; Curtis, S.; Matchett, M. D.; Yeung, H.;

Sweeney, M. I.; et al. MALDI-TOF MS characterization of proanthocyanidins from cranberry fruit (*Vaccinium macrocarpon*) that inhibit tumor cell growth and matrix metalloproteinase expression in vitro. *J. Sci. Food Agric.* **2006**, *86*, 18−25.
(31) Tóth, G.; Alberti, Á.; Sólyomváry, A.; Barabás, C.; Boldizsár, I.; Noszál, B. Phenolic profiling of various olive bark-types and leaves: HPLC-ESI/MS study. *Ind. Crops Prod.* **2015**, *67*, 432−438.
(32) Wu, X.; Prior, R. L. Systematic identification and characterization of anthocyanins by HPLC-ESI-MS/MS in common foods in the United States: Fruits and berries. *J. Agric. Food Chem.* **2005**, *53*, 2589−2599.
(33) Sun, J.; Lin, L. Z.; Chen, P. Study of the mass spectrometric behaviors of anthocyanins in negative ionization mode and its applications for characterization of anthocyanins and non-anthocyanin polyphenols. *Rapid Commun. Mass Spectrom.* **2012**, *26*, 1123−1133.
(34) Wang, Y.; Yang, C.; Li, S.; Yang, L.; Wang, Y.; Zhao, J.; Jiang, Q. Volatile characteristics of 50 peaches and nectarines evaluated by HP-SPME with GC-MS. *Food Chem.* **2009**, *116*, 356−364.
(35) Sampaio, B. L.; Edrada-Ebel, R.; Da Costa, F. B. Effect of the environment on the secondary metabolic profile of *Tithonia diversifolia*: A model for environmental metabolomics of plants. *Sci. Rep.* **2016**, *6*, 29265.
(36) Okazaki, Y.; Kamide, Y.; Hirai, M. Y.; Saito, K. Plant lipidomics based on hydrophilic interaction chromatography coupled to ion trap time-of-flight mass spectrometry. *Metabolomics* **2013**, *9*, 121−131.
(37) Mehl, F.; Marti, G.; Boccard, J.; Debrus, B.; Merle, P.; Delort, E.; Baroux, L.; Raymo, V.; Velazco, M. I.; Sommer, H.; et al. Differentiation of lemon essential oil based on volatile and non-volatile fractions with various analytical techniques: A metabolomic approach. *Food Chem.* **2014**, *143*, 325−335.
(38) Petrakis, E. A.; Cagliani, L. R.; Polissiou, M. G.; Consonni, R. Evaluation of saffron (*Crocus sativus* L.) adulteration with plant adulterants by1H NMR metabolite fingerprinting. *Food Chem.* **2015**, *173*, 890−896.
(39) Chen, P.; Luthria, D.; Harrington, P. D. B.; Harnly, J. M. Discrimination among panax species using spectral fingerprinting. *J. AOAC Int.* **2011**, *94*, 1411−1421.

DOI: 10.1021/acs.jafc.8b05029
J. Agric. Food Chem. 2018, 66, 12206−12216